INTERNAL GRAVITY WAVES ACTIVITY HOTSPOT AND IMPLICATIONS FOR THE MIDDLE ATMOSPHERIC DYNAMICS

Petr Šácha[(1)], Petr Pišoft[(1)], Friederike Lilienthal[(2)], Christoph Jacobi[(2)]

[(1)] Charles University in Prague, Faculty of Mathematics and Physics, Department of Atmospheric Physics, V Holešovičkách 2, Praha 8, 180 00, Czech Republic, Email: petr.sacha@mff.cuni.cz
[(2)] Institute for Meteorology, University of Leipzig, Stephanstr. 3, D-04103 Leipzig, Germany

ABSTRACT

Internal gravity waves are widely recognized to contribute significantly to the energy and angular momentum transport. They play a significant role in affecting many of the middle atmospheric phenomena (like the QBO or Brewer-Dobson circulation). Using GPS RO density profiles, we have discovered a localized area of enhanced IGW activity and breaking in the lower stratosphere of Eastern Asia/North-western Pacific region.

With a 3D primitive equation model of the middle atmosphere we studied the effects of such a localized breaking region on large-scale dynamics and transport. Possible forcing and propagation directions of planetary waves caused by such a localized IGW forcing were investigated and consequences for the polar vortex stability and stratosphere-troposphere exchange in the tropical region were discussed.

Finally, applying 3D EP flux and 3D residual circulation diagnostics, we investigated the possible role of this area in the longitudinal variability of the Brewer-Dobson circulation with a hypothesis of its enhanced downwelling branch in this region. In the proces, model results were compared with the ozone and tracer distribution data from GOME, GOMOS, MIPAS and SCIAMACHY further confirming the importance of the Eastern Asia/North-western Pacific region for middle atmospheric dynamics.

1. INTRODUCTION

Gravity waves in geophysical fluid dynamics are usually described as a group of wave motions where the restoring force is the gravity. Internal gravity waves (IGW) as a part of them are of special importance in the atmosphere where they are a naturally occurring and a ubiquitous phenomenon. IGW affect the atmospheric composition, circulation, and dynamics. In general, they contribute to restore the equilibrium and to gain energetically more favourable conditions.

Understanding the IGW related processes is essential for a proper description and modelling of the middle and upper atmospheric dynamics (as reviewed comprehensively by [1]). In recent years, IGW were acknowledged to play a role in some of the most challenging atmospheric topics. Examples are the influence on the (middle atmospheric) climate change and possible acceleration of the Brewer-Dobson circulation (BDC) (e.g., [2]), the role for the formation of the Quasi-Biennial Oscillation (QBO) ([3]) or the influence on the stratosphere-troposphere exchange (STE) ([4]).

IGWs exhibit a broad distribution of spatial and temporal scales and they need to be parameterized in atmospheric and climate models. Despite significant advances in our understanding of IGW and their effects in the past few decades, observational constraints on IGW parameterizations are still sorely lacking as noted by [5]).

In this paper we are presenting an IGW activity and breaking hotspot in the Eastern Asia/North-western Pacific region and show some preliminary results of the numerical model experiments that support our hypothesis that this hotspot can play a significant role in the middle atmospheric circulation and dynamics.

The paper is structured as follows: the technique of IGW analysis from the GPS RO data, numerical model and trace gas datasets description are given in section 2. Section 3 is divided into three parts: in the first part a discovery of the IGW hotspot is presented with a subsequent discussion of potential energy of disturbances as a proxy for IGW activity, in the second part possible dynamical consequences of this hotspot are shown and in the third part our hypothesis is confronted with distributions of some selected trace gases. Discussion and summary are given in the section 4.

2. METHODOLOGY

For analysis of the IGW activity we used L2 level FORMOSAT-3/COSMIC data from 2007 to 2010. We used GPS RO density profiles gridded on a 3° × 3° grid ranging from tropopause up to the 35 km altitude following [6]. In [6] advantages of using density rather than dry temperature profiles (e.g. inclusion of nonhydrostatic IGW) are also listed. As a proxy for wave activity we are using usual potential energy density of disturbances per unit mass (*Ep*) computed using the formula provided by [7].

To access the stability of the wave field we exploit gradient Richardson following [8] to access a dynamical instability of the wave field and a maximum growth rate

of disturbances to access Rayleigh-Taylor convective instability as expressed e.g. in [9].

For the investigation of possible dynamical consequences of the IGW hotspot we run a nonlinear 3D mechanistic global circulation model named Middle and Upper Atmosphere Model (MUAM). It has a horizontal resolution of 5° × 5.625° and extends in 56 vertical layers up to an altitude of 160 km in log-pressure height as described in detail by [10]).

We have performed a set of experimental runs to study the influence of a localised IGW hotspot on middle atmospheric circulation and dynamics. The runs are described in detail in [11].

In this paper we show results from runs for November and January conditions with latitudinal/longitudinal dependent IGW amplitude weights as an input for the MUAM IGW parametrization scheme. These weights are obtained from *Ep* calculated from GPS RO density profiles as described by [12]. The GW weights are calculated from these data by dividing *Ep* at each grid point by the global mean potential energy. The *Ep* values refer to an average between tropopause and 35 km altitude. With this approach we are ensuring better geographical representation of IGW activity.

The vertical structure and longitudinal variability of the residual circulation from MUAM runs are compared with zonal cross sections of distribution of selected trace gases computed from 3D assimilated nadir ozone profiles from GOME and GOME-2 observations developed by Royal Netherlands Meteorological Institute (KNMI) within the ozone project of the CCI programme of European Space Agency and N_2O, CO, H_2O volume mixing ratio profiles from the Michelson Interferometer for Passive Atmospheric Sounding (MIPAS) V5R data produced by Karlsruhe Institute of Technology, Institute of Meteorology and Climate Research - Atmospheric Trace Gases and Remote Sensing (KIT IMK/IAA).

Further, to show the robustness of our claim of an enhanced branch of BDC in the EA/NP region we computed the thirty-year annual cycle average of Multi Sensor Reanalysis of Ozone (MSR) total ozone column field from 1978 to 2008. MSR is produced by KNMI from TOMS (on the satellites Nimbus-7 and Earth Probe), SBUV (Nimbus-7, AA-9, NOAA-11 and and NOAA-16), GOME (ERS-2), SCIAMACHY (Envisat), OMI (EOS-Aura), and GOME-2 (Metop-A) data.

3. RESULTS

3.1. Analysis of geographical and seasonal distribution of IGW activity and effects

In this subsection we are giving a summary of results presented in [12]. Analyzing the distribution of *Ep* they found, in average, a distinguished region of high IGW activity in autumn, winter and partly in spring and of maximal values in the Northern Hemisphere in October and November (see Fig. 1). This area is significant starting from the 70 hPa level up to the 6 hPa level.

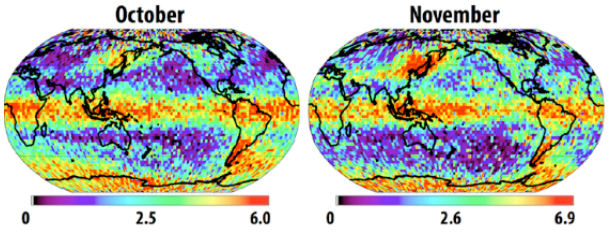

Figure 1. Monthly means of the potential energy in J/kg averaged across the whole vertical profile for the studied time period 2007-2010.

Values and distributions of the wave breaking indicators, Richardson number (see Fig. 2) and convective instability growth rate (not shown), are further accentuating the importance of the studied area. The NP/EA hotspot is a dominant feature in the maps across all the levels even in spring and winter months (when *Ep* in this region is not dominant across the NH). Overall, the results are suggestive of vertically robust and long lasting breaking of IGWs in this region.

The different distribution of wave breaking and wave activity hotspots in space and time can partly be a consequence of inappropriateness of usage of *Ep* as a wave activity proxy, which can lead to under (or over) estimations of wave activity depending on the prevailing IGW spectrum. The point is that for IGW in a rotating frame the equipartitioning between potential and kinetic energy doesn't hold and their ratio is dependent on the wave frequency. This is discussed in detail in [12].

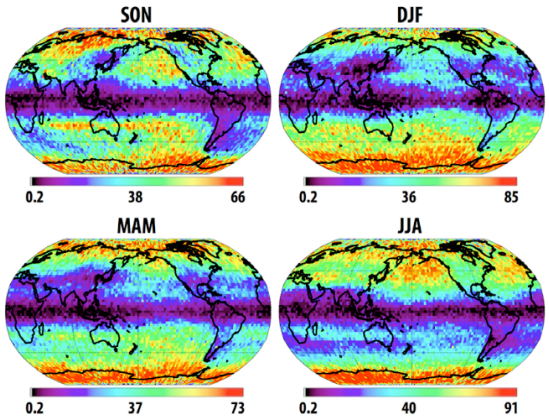

Figure 2. Seasonal means of the gradient Richardson number averaged across the whole vertical profile for the studied time period 2007-2010.

Reference [12] using reanalysis data found an area of specific dynamics (e.g. region of highest temperatures in the NH lower stratosphere in autumn and winter) and of low annual cycle amplitude in the stratosphere in the NP/EA region. The working hypothesis is that this dynamical anomaly is connected with a specific IGW activity over this region.

Reference [12] also gives a discussion of possible wave sources contributing to a IGW spectrum in this region. In short, they found that there are low values of cumulative wind rotation above NP/EA favorable for vertical propagation of orographic waves (phase speed equal to zero). And also prevailing surface winds are suggestive of orographic creation of IGW due to the topography of Japan, Sachalin, Korean Peninsula and eastern Asia coastline. Another source can be a convective activity connected with the Kuroshio current in autumn, Doppler shifting due to the strong winds (jet stream location at the western boundary of the region) and possibly some in situ wave generation in the upper troposphere/lower stratosphere ([13]) – subtropical and polar jet stream merging).

3.2. Longitudinal variability of BDC and planetary waves sourcing

In a model study, [11] compared an influence of different distributions of the IGW amplitudes (as an input for the MUAM IGW parametrization scheme) based on artificial values (reference) and GPS RO data on the global climatology. They found significant differences in many aspects of the middle atmospheric January circulation (e.g. strength of the polar vortex and BDC) and also in planetary waves (PW) amplitude and propagation directions (Fig. 3).

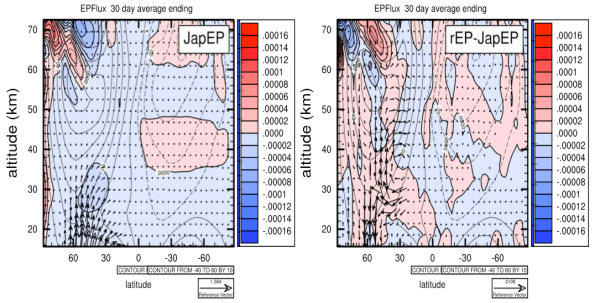

Figure 3. Left: Mean E-P flux and its divergence per unit mass from GPS RO based IGW weights run for January conditions, contours show mean zonal wind. Right: Difference between reference and GPS RO based run. Arrows are scaled according to the relative ranges of the plot axes.

In Fig. 3 a comparison is shown between the reference run and GPS based (called JapEP in Fig. 3) run for January conditions. 2D Eliassen-Palm flux (E-P) analysis reveals stronger PW propagation in the lower stratosphere from the midlatitudes equatorward and along the edge of a polar vortex. In future work we will investigate to what degree these PW can be generated by the localised IGW activity and hotspot in the NP/EA region.

The theoretical possibility of PW forcing by IGW was numerically analysed e.g. by [14] and experimentally verified by [15] for the mesosphere. In the case of the detected IGW hotspot, the IGW breaking is observed starting already around 20 km and there might be ongoing a unique in situ PW generation taking place already in the lower stratosphere (LS). Reference [16] observed equatorially propagating planetary waves in the LS and argued that they can play an important role in the stratospheric-tropospheric exchange (STE). Such a mechanism is supported by results from [17] indicating that the longitude of maximal passage of tropical air into the stratosphere in autumn corresponds to the region of our interest. Reference [18] identified an area south/southeast of the region of interest to have maximum tropopause fold frequency in NH winter. Reference [19] used back trajectories driven by analyzed large-scale wind fields to investigate troposphere to stratosphere transport (TST) and found, particularly in autumn, a region of significant transport south of the region of interest. Indeed, in Fig. 3 we can see enhanced equatorward propagation and stronger E-P flux convergence in the tropics in the run with better geographical representation of IGW.

In the Fig. 3, as written before, one can also see enhanced PW propagation along the edge of a polar vortex in the LS region and enhanced convergence both inside and outside of the vortex up to 40 km. These PW may influence the stability of the polar vortex and in future work we intend to study their influence on the sudden stratospheric warming (SSW) occurrence.

There is an agreement in the literature on the role of wave activity in preconditioning SSW ([20]). Most attention is paid to the role of upward propagating PW in preconditioning SSW ([21], [22], [23]), but there is also growing evidence about the enhancement of IGW amplitudes prior to SSW ([24], [5]). We intend to analyze the potential of the IGW hotspot to contribute to the preconditioning of SSW directly and indirectly due to the generation of Rossby waves.

Consequences of the IGW hotspot for the longitudinal variability of the BDC were studied by means of 3D residual circulation according to algorithms provided by [25]. Application on data from the GPS based MUAM run reveals that there is enhanced downwelling above the NP/EA region penetrating to lower levels than elsewhere (see Fig. 4). Note the migration of the area of maximum subsidence with height to the northwest towards the region of eastern Siberia, where it was diagnosed by [26].

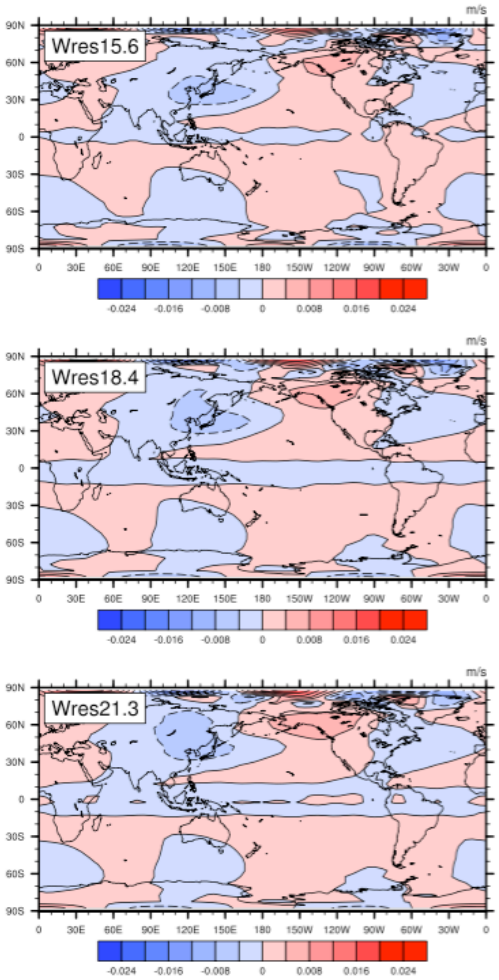

Figure 4. Geographical distribution of the residual vertical velocity on three consequent model levels in the LS region (log-pressure height of 15.6 km, 18.4 and 21.3 km).

One has to have in mind this migration of the subsidence area with height when contrasting the residual circulation with total column distributions of tracers (Fig. 5). Also, the residual velocities are closely related to Lagrangian-mean velocities up to the $O(\alpha^2)$ only for small amplitude steady waves ([27]). Reference [28] gave a consistent theoretical background and a comprehensive manual how to get approximation for Lagrangian-mean velocities also for unsteady waves. We intend to use this approach in future work.

Nevertheless, from comparison of the model results (Fig.4) with thirty-year average of MSR total ozone column field in January, we can see with regard to the preceding discussion that the MUAM results are realistic and also the enhanced branch of BDC above NP/EA is a robust feature influencing significantly ozone concentrations in midlatitudes.

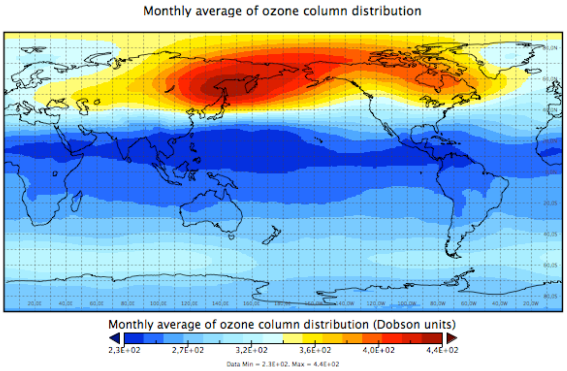

Figure 5. Mean total ozone column distribution computed from MSR in January (1978-2008).

3.3. Comparison with trace gases distributions

Zonal cross-section of MUAM vertical residual velocity gives us an interesting insight into the structure of the residual circulation.

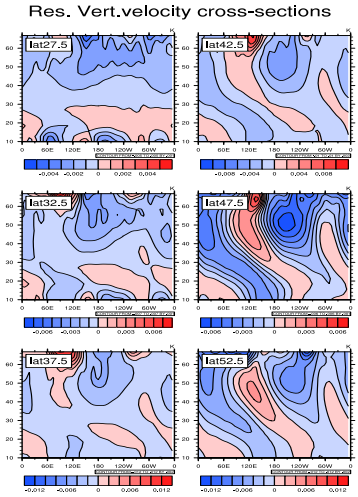

Figure 6. Zonal cross-sections at latitudes around 35°N of MUAM residual vertical velocity in November.

In Fig. 6 we can see that from roughly 40°N the vertical residual velocity field is dominated by PW2 with the maximum subsidence branch penetrating to the lower stratosphere in the EA/NP region. Ridges and troughs of the wave show a characteristic westward tilt with height, which was already discussed in subsection 3.2.

Comparison of MUAM results and trace gases distributions confirms a realistic behavior of the model middle atmospheric circulation. From approximately 35°N we can see evidence (Fig. 7, 9, 10) of the enhanced branch of BDC above NP/EA region reaching the lowest levels around 140°E (compare with location of IGW activity hotspot).

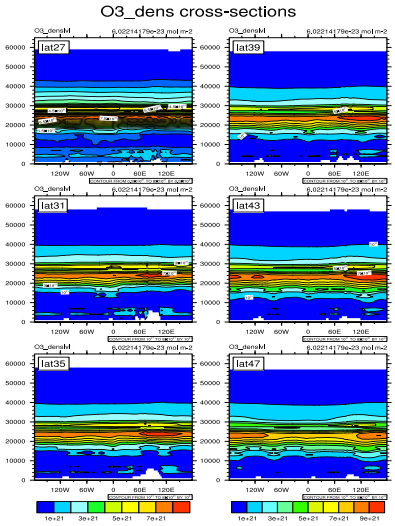

Figure 7. As in Fig. 6 but for the November 1997-2008 mean of O_3 mole content in an atmospheric layer.

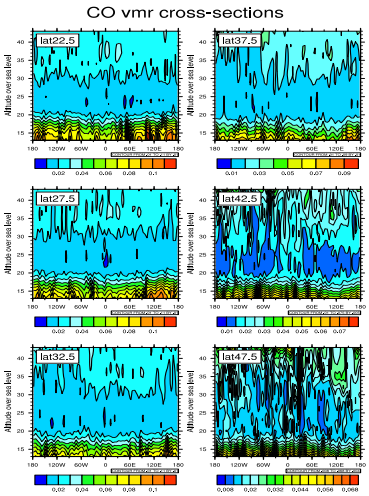

Figure 8. As in Fig. 6 but for the November 2009 volume mixing ratio of CO.

On the other hand around 150°E we can see in the fields of H_2O and N_2O (Fig. 9 and 10) signatures of upwelling of lower stratospheric air higher into the stratosphere. The other two peaks of PW2 are not pronounced in tracer distributions.

From the distribution of *CO* (Fig. 8) we find that the tropopause (chemical) is located at lower altitudes above NP/EA region than at other longitudes starting roughly from 35°N. Note also the local maxima of *CO* concentrations around 15 km altitude between 27.5 and 37.5°N and around 130°E, as they are located above the ocean (no artificial sources) this raises the question whether they can be considered as signatures of STE.

Another interesting feature can be seen in Fig. 7 from 31°N to 35°N - the maximum of the ozone mole content is located above the Himalayas. We have no explanation for this feature yet but we take it as a suggestion not to forget the possible role of Himalayas in future studies of EA/NP IGW hotspot and its dynamical implications.

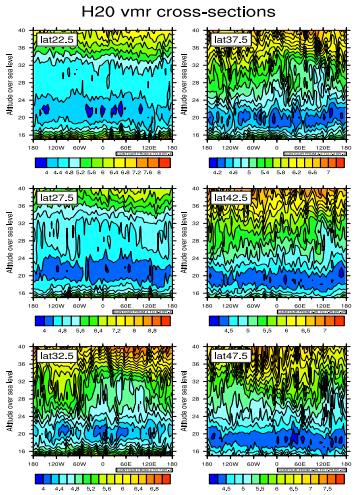

Figure 9. As in Fig. 6 but for the November 2009 volume mixing ratio of H_2O.

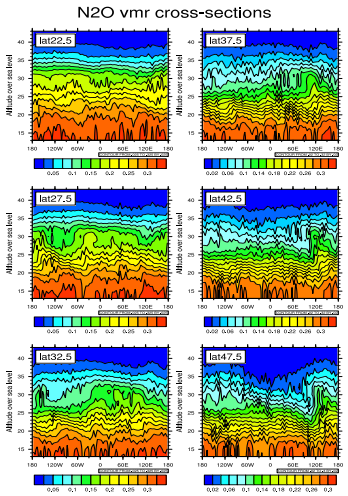

Figure 10. As in Fig. 6 but for the November 2009 volume mixing ratio of N_2O.

4. SUMMARY AND CONCLUSIONS

Using GPS RO data we have found high IGW *Ep* values while static and dynamic stability indicators suggest massive wave breaking in the EA/NP region (details in [12]). 2D E-P flux diagnostics of MUAM runs reveals enhanced equatorward and poleward propagation of planetary waves, if the IGW hotspot area is included (GPS RO based input for MUAM IGW parametrization scheme, details in [11]). This finding can possibly have consequences for STE and polar vortex dynamics.
Distributions of trace gases and 3D analysis of MUAM runs are pointing to robust downwelling of equatorial air masses (enhanced branch of Brewer-Dobson circulation) reaching deeper in the NP/EA region stratosphere than elsewhere. But the causality and time evolution on seasonal as well as interannual scale is unclear and may be the product of wave mean flow interactions and induced residual circulation in a complex three dimensional system with feedback mechanisms involved.

5. REFERENCES

1. Fritts, D. C. and Alexander, M. J.: Gravity wave dynamics and1085 effects in the middle atmosphere, Reviews of Geophysics, 41, doi:10.1029/2001RG000106, http://dx.doi.org/10.1029/ 2001RG000106, 2003.

2. Garcia, R. R. and Randel, W. J.: Acceleration of the Brewer-Dobson circulation due to increases in greenhouse gases, Journal of the1090 Atmospheric Sciences, 65, 2731–2739, 2008.

3. Ern, M., Ploeger, F., Preusse, P., Gille, J. C., Gray, L. J., Kalisch,1065 S., Mlynczak, M. G., Russell, J. M., and Riese, M.: Interaction of gravity waves with the QBO: A satellite perspective, Jour- nal of Geophysical Research: Atmospheres, 119, 2329–2355, doi:10.1002/2013JD020731, 2014.

4. Kunkel, D., Hoor, P., & Wirth, V. (2014). Can inertia-gravity waves persistently alter the tropopause inversion layer? *Geophysical Research Letters*, n/a–n/a. doi:10.1002/2014GL061970.

5. Wang, L. and Alexander, M.: Global estimates of gravity wave pa-rameters from GPS radio occultation temperature data, Journal of Geophysical Research: Atmospheres (1984–2012), 115, 2010.

6. Šácha, P., Foelsche, U., and Pišoft, P.: Analysis of internal gravity waves with GPS RO density profiles, Atmospheric Measurement Techniques, 7, 4123–4132, doi:10.5194/amt-7-4123-2014, http: //www.atmos-meas-tech.net/7/4123/2014/, 2014.

7. Wilson, R., Chanin, M., and Hauchecorne, A.: Gravity waves in the middle atmosphere observed by Rayleigh lidar: 2. Clima- tology, Journal of Geophysical Research: Atmospheres (1984–2012), 96, 5169–5183, 1991.

8. Senft, D. C. and Gardner, C. S.: Seasonal variability of gravity wave activity and spectra in the mesopause region at Urbana, Journal of Geophysical Research, 96, 17229, doi:10.1029/91JD01662, http://doi.wiley.com/10.1029/91JD01662, 1991.

9. Sutherland, B. R.: Internal gravity waves, Cambridge University Press, 2010.

10. Pogoreltsev, A. I., Vlasov, A. A., Fröhlich, K., and Jacobi, C. (2007). Planetary waves in coupling the lower and upper atmosphere. *J. Atmos. Solar-Terr. Phys.*, 69:2083–2101.

11. Lilienthal, F., P. Šácha and Ch. Jacobi, 2015: Gravity Wave effects on a Modeled Mean Circulation, Rep. Inst. Meteorol. Univ. Leipzig, in press.

12. Šácha, P., Kuchař, A., Jacobi, C., and Pišoft, P (2015).: Enhanced internal gravity wave activity and breaking over the Northeastern Pacific / Eastern Asian region, *Atmos. Chem. Phys.*, submitted, http://acp.pisoft.cz/2015-1/

13. Mohri, K.: On the fields of wind and temperature over Japan and adjacent waters during winter of 1950–1951, Tellus, 5, 340–358,1953.

14. Smith, A. K.: The origin of stationary planetary waves in the up- per mesosphere, Journal of the atmospheric sciences, 60, 3033– 3041, 2003.

15. Lieberman, R. S., D. M. Riggin, and D. E. Siskind (2013), Stationary waves in the wintertime mesosphere: Evidence for gravity wave filtering by stratospheric planetary waves, *J. Geophys. Res. Atmos*., 118, 3139–3149, doi:10.1002/jgrd.50319.

16. Ortland, D. A.: Rossby wave propagation into the tropical strato- sphere observed by the High Resolution Doppler Imager, Geo- physical research letters, 24, 1999–2002, 1997.

17. Riese, M., Oelhaf, H., Preusse, P., Blank, J., Ern, M., Friedl/Vallon, F., Fischer, H., Guggenmoser, T., Höpfner, M., Hoor, P., and Others: Gimballed Limb Observer for Radiance Imaging of the Atmosphere (GLORIA) scientific objectives, Atmospheric Measurement Techniques, 7, 1915–1928, 2014.

18. Škerlak, B., M. Sprenger, S. Pfahl, E. Tyrlis, and H. Wernli (2015), Tropopause folds in ERA-Interim: Global climatology and relation to extreme weather events, J. Geophys. Res. Atmos., 120, doi: 10.1002/2014JD022787.

19. Berthet, G., Esler, J. G., and Haynes, P. H.: A Lagrangian per- spective of the tropopause and the ventilation of the low- ermost stratosphere, Journal of Geophysical Research, 112, D18102, doi:10.1029/2006JD008295, http://doi.wiley.com/10. 1029/2006JD008295, 2007.

20. Baldwin, M. P., and T. J. Dunkerton, 2001: Stratospheric harbingers of anomalous weather regimes. *Science*, 294, 581–584.

21. Nishii, K., Nakamura, H. Miyasaka, T. (2009). Modulations in the planetary wave field induced by upward propagating Rossby wave packets prior to stratospheric sudden warming events: A case study. *Quarterly Journal of the Royal Meteorological Society*, 135(638), 39-52.

22. Hoffmann, P., Singer, W., Keuer, D., Hocking, W. K., Kunze, M., and Murayama, Y. (2007). Latitudinal and longitudinal variability of mesospheric winds and temperatures during stratospheric warming events. *J. Atmos. Solar-Terr. Phys*., 69:2355–2366.

23. Alexander, S. P., & Shepherd, M. G. (2010). Planetary wave activity in the polar lower stratosphere. *Atmospheric Chemistry and Physics*. doi:10.5194/acp-10-707-2010

24. Ratnam, M.V., T. Tsuda, Ch. Jacobi, and Y. Aoyama, 2004a: Enhancement of gravity wave activity observed during a major Southern Hemisphere stratospheric warming by CHAMP/GPS measurements. *Geophys. Res. Lett*. 31, L16101, doi:10.1029/2004GL019789.

25. Kinoshita, T., & Sato, K. (2013). A formulation of three-dimensional residual mean flow applicable both to inertia–gravity waves and to Rossby waves. *Journal of the Atmospheric Sciences*, *70*(6), 1577-1602.

26. Demirhan Bari, D., Gabriel, a., Körnich, H., and Peters, D. W. H.: The effect of zonal asymmetries in the BrewerDobson cir culation on ozone and water vapor distributions in the northern middle atmosphere, *Journal of Geophysical Research*: At 980 mospheres, 118, 3447–3466, doi:10.1029/2012JD017709, 2013.

27. Bühler, O.: Waves and mean flows, Cambridge University Press, 2014.

28. Noda, A.: Generalized Transformed Eulerian Mean (GTEM) De- scription for Boussinesq Fluids, Journal of the Meteorological Society of Japan. Ser. II, 92, 411–431, doi:10.2151/jmsj.2014- 501, http://jlc.jst.go.jp/DN/JST.JSTAGE/jmsj/2014-501?lang=1175 en&from=CrossRef&type=abstract, 2014.